Efficient out-coupling and beaming of Tamm optical states via surface plasmon polariton excitation

Cite as: Appl. Phys. Lett. **104**, 231116 (2014); https://doi.org/10.1063/1.4882180
Submitted: 24 April 2014 . Accepted: 28 May 2014 . Published Online: 11 June 2014

M. Lopez-Garcia, Y.-L. D. Ho, M. P. C. Taverne, L.-F. Chen, M. M. Murshidy, A. P. Edwards, M. Y. Serry, A. M. Adawi, J. G. Rarity, and R. Oulton

Efficient out-coupling and beaming of Tamm optical states via surface plasmon polariton excitation

M. Lopez-Garcia,[1] Y.-L. D. Ho,[1] M. P. C. Taverne,[1] L.-F. Chen,[1] M. M. Murshidy,[2,3,4] A. P. Edwards,[2] M. Y. Serry,[4] A. M. Adawi,[2] J. G. Rarity,[1] and R. Oulton[1]
[1]*Department of Electrical and Electronic Engineering, University of Bristol, Faculty of Engineering, Queen's Building, University Walk, Bristol BS8 1TR, United Kingdom*
[2]*Department of Physics and Mathematics, University of Hull, Cottingham Road, HU6 7RX Hull, United Kingdom*
[3]*Department of Physics, Faculty of Science, Helwan University, Helwan, Egypt*
[4]*Yousef Jameel Science and Technology Research Center, The American University in Cairo, Egypt*

(Received 24 April 2014; accepted 28 May 2014; published online 11 June 2014)

We present evidence of optical Tamm states to surface plasmon polariton (SPP) coupling. We experimentally demonstrate that for a Bragg stack with a thin metal layer on the surface, hybrid Tamm-SPP modes may be excited when a grating on the air-metal interface is introduced. Out-coupling via the grating to free space propagation is shown to enhance the transmission as well as the directionality and polarization selection for the transmitted beam. We suggest that this system will be useful on those devices, where a metallic electrical contact as well as beaming and polarization control is needed. © *2014 AIP Publishing LLC*. [http://dx.doi.org/10.1063/1.4882180]

Optical Tamm states are the electromagnetic equivalent of modes confined to surface states for electrons originally described by Tamm.[1] This type of resonance takes place, for example, at the surface of a truncated photonic crystal[2] or at the interface between two periodic dielectric structures that show a band gap in frequency.[3] Recent developments have shown that Tamm plasmons (TPs) may be generated at the interface between a metal and a distributed Bragg reflector (DBR) for frequencies within the photonic band gap.[4,5] The simplicity of the structure of such systems combined with their good optical performance has attracted much attention. Applications, such as transmission enhancement through nanoholes,[6] optical switching,[7] lasing,[8] or single photon emission,[9] have already being demonstrated. In addition, the interaction of TPs with other type of resonances, such as localized modes in a cavity, has been studied.[10] Surface plasmon polaritons (SPPs), on the other hand, are surface waves intrinsic to any metallic layer showing strong field confinements in small volumes. The ability to combining these properties therefore motivates the study of hybrid TP-SPP systems. However, while TPs may be excited for wave vectors within the air-light cone, SPP modes are forbidden for that dispersion region,[11] implying that TP-SPP momentum matching cannot be fulfilled. Recently, however, it has been demonstrated that hybrid modes between Tamm states and SPPs may be excited outside of the light cone using a prism-coupling approach,[12] with light incident from the DBR face of the system. Although the physics involved in this particular configuration is interesting, technological exploitation of Tamm-SPP hybrid modes will likely require more integrated excitation techniques. Some approaches to TP-SPP coupling via structuring the metal have been proposed.[13–15] However, this has only been realised within the THz regime[16] or using complex implementations.[17]

In this paper, we present a relatively simple TP-SPP coupling structure suitable for the visible to near-infrared spectral range. We incorporate a grating of period Λ into a 120 nm layer of gold that sits on the top surface of a nine pair of a Si_3N_4/SiO_2 DBR structure, as illustrated in Fig. 1(a). By exciting Tamm resonances through the DBR side of the structure, we demonstrate that Tamm-SPP coupling is manifest for the wavelength-fulfilling momentum matching condition between TP and SPP modes. Simulations and analytical models support our measurements with very good agreement. In addition, we demonstrate that a strong transmission enhancement (16 times in our case) is obtained when compared with the metal-DBR structure without grating. Angle- and polarization-resolved transmission spectroscopy shows excellent agreement with dispersion relation calculations of the different modes, including a strong directionality of the transmitted beam. The results presented in this work demonstrate a simple method for the excitation of processes where transmission enhancement and polarization control is of interest such as in extraordinary transmission[18] or spin-orbit interaction[19] phenomena. In particular, TP-SPP hybrid modes would be useful in devices where coupling to the SPP is commonly very inefficient and requires complex fabrication approaches such as structuring both sides of the metallic membrane.[20,21]

Figure 1(a) shows a schematic of the structure under study, in this work. With the appropriate structural parameters, this system supports a TP mode at the metal-DBR interface. The TP mode may be excited with an external beam incident through the DBR side for both p- and s-polarizations.[4] In addition, a SPP propagates at the metal-air interface. For a non-structured metal-air interface, the coupling condition between TP and SPPs cannot be fulfilled within the light cone.[12] When a grating is included, coupling to the SPP becomes possible through illumination from free space, and TP-SPP coupling can therefore also be achieved using the appropriate grating period. The dispersion relation as a function of the incident angle for the TP and SPP for bulk Au/air interface[22] is shown in Figure 2(a). The optical constants of the materials used in the calculations were extracted from literature.[22] The empty

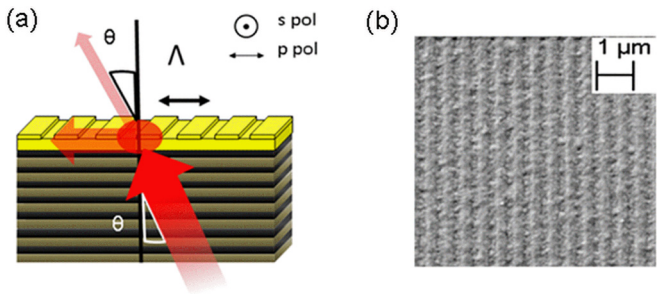

FIG. 1. (a) Diagram for the structure studied, indicating illumination configuration for transmission measurements. (b) Scanning Electron Microscope (SEM) image of the surface of a Si_3N_4/SiO_2 DBR coated with a 120 nm Au film into which has been etched a grating of depth 30 nm and grating period $\Lambda = 600$ nm.

lattice model[23] was used to calculate the folding of the SPP dispersion relation according to the period of the grating. For convenient comparison with the experimental results, dispersion curves for SPP and TP are shown as a function of incident angle. For the particular case of the SPP modes, we consider conservation of the parallel component of the incident wavevector (k_{in}^{II}).[24] In this case, $k_{in}^{II} = k_0 \sin\theta_{in}$ and $k_{in}^{II}(\omega) = k_{SPP}(\omega) \pm m|G|$ with $k_{SPP}(\omega)$ being the dispersion relation of the SPP mode in the flat metal/air interface, m is an integer number (m = 0, ±1,..) representing the diffraction order and $|G| = 2\pi/\Lambda$ being the lattice vector of the grating. The dispersion relation for the TP modes was calculated numerically using a commercial finite difference time domain (FDTD) tool.[25] Regardless of a more detailed study of the TP to SPP coupling process, we assume the simple approximation that phase matching between TP and SPP occurs when $k_{TP}(\omega) = k_{SPP}(\omega)$, where $k_{TP/SPP}$ are the parallel components of the wavevector for the Tamm and SPP, respectively. It is therefore evident that TP and SPP momentum matching may be tuned to a wide range of desired incident angles and wavelengths through control of the periodicity of the grating.

Dashed and dotted lines in Figure 2(a) show the dispersion relations for the SPP at Air/Au interface with grating pitch $\Lambda = 500$ and 600 nm. An infinitely thick metal layer is considered in order to avoid hybrid plasmonic modes due to plasmon excitation at both sides of the metal film. Notice that no DBR is considered in this case. Diffraction orders m = ±1, ±2 were considered in the empty lattice model to calculate the final SPP dispersion relation in the system. The solid line in the same plot shows the dispersion for TP modes without grating. It may be observed that for $\Lambda = 600$ nm, SPP-TP coupling takes place at $\lambda = 710$ nm and at $\theta_{in} \approx 8°$, whereas for $\Lambda = 500$ nm coupling takes place at $\lambda \approx 700$ nm and $\theta_{in} \approx 21°$. Although numerical calculations may be performed for any particular case, we consider the situation at which coupling happens at normal incidence. In this case, an approximate analytical expression to determine the TP-SPR matching wavelength may be deduced. If the expressions for resonant wavelengths of Tamm[4] and SPP[11] are considered separately, it is easily found that the coupling at normal incidence takes place when

$$m\frac{2\pi c}{\Lambda}\left(\frac{\varepsilon_m + \varepsilon_1}{\varepsilon_m \varepsilon_1}\right)^{1/2} \approx \omega_c\left(1 + \frac{2n_a\omega_c}{\sqrt{\varepsilon_b}\beta\omega_c}\right)^{-1} \quad (1)$$

with $\beta = \pi n_a/|n_a - n_b|$, n_a, n_b being the refractive index of the two materials of the DBR, with $n_a > n_b$. Λ is the period of the grating and c is the speed of light in vacuum. ω_c is the central frequency of the $\lambda/4$ DBR and ω_p is the plasma frequency of the metal under consideration. ε_b is the background dielectric constant for the metal in the Drude model approximation. Finally, $\varepsilon_{m,1}$ are the real part of the dielectric constant for metal and dielectric on the SPP surface of our structure, respectively, in this case, Au and air.

To evaluate the validity of the coupling model elaborated so far, Fig. 2(b) shows an FDTD calculation of the field intensity (normalized by source intensity in air at the same position) for $\Lambda = 500$ nm and 600 nm with p-polarized plane-wave illumination at $\lambda = 710$ nm and $\theta_{in} = 5°$. It may be observed that, for both periods, a strong field confinement is obtained at the TP region (metal-DBR interface). However, for $\Lambda = 600$ nm only, a high field intensity is apparent at the grating side of the metal. This appearance is in agreement with the dispersion relations in Fig. 2(a), as no TP-SPP phase matching occurs for $\Lambda = 500$ nm at $\theta_{in} = 5°$.

It has been noted that using a grating as the TP-SPP coupler also allows the SPP to be coupled to radiative modes in air. If we therefore consider the case where light is incident from air onto the DBR side of the structure, an enhanced transmission is expected for the wavelengths at which the TP-SPP coupling occurs. This phenomenon should be differentiated from the resonant optical transmission obtained in Tamm plasmon structures with non-structured gold-air interface.[26,27] The grey line in Fig. 2(c) shows the calculated transmission through the structure without a grating. It may be observed that at the TP resonant wavelength

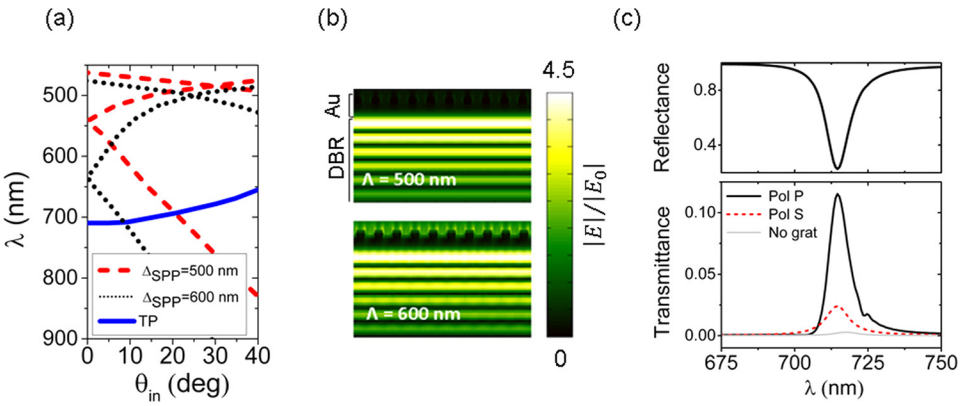

FIG. 2. (a) Dispersion relations for TP (blue solid line) and SPP at the grating (Au)/air interface, with periods $\Lambda = 500$ nm (red dashed) and 600 nm (black dotted). (b) Electric field intensity distribution inside the structure after illumination through DBR for periods in (a), $\theta_{in} = 5°$ and $\lambda = 710$ nm. (c) Calculated reflectance and transmission of the TP only (grey solid line) and TP-SPP structure (black solid and red dotted lines) with $\Lambda = 600$ nm and $\theta_{in} = 5°$.

($\lambda = 710$ nm), the transmission value is as low as 7×10^{-3}. Therefore, we will use the structure without a grating as a reference for calculating the enhancement in transmission obtained due to the TP-SPP coupling. It is convenient for further comparison with experiments to define the enhanced transmission parameter $\gamma = T_{TP-SPP}/T_{TP}$, where T_{TP-SPP} and T_{TP} are the transmissions for the same metal-DBR structures, evaluated at the same wavelength, with and without grating, respectively.

Figure 2(c) also shows the calculated reflectance and transmission (T_{TP-SPP}) for a grating of $\Lambda = 600$ nm at $\theta_{in} = 5^\circ$ for p- and s-polarized incident light. As presented in Figs. 2(a) and 2(b), this configuration allows TP-SPP coupling for p-polarised light only. Hence, high transmission is obtained at resonant wavelength $\lambda = 710$ nm. The enhancement in transmission in this case is as high as $\gamma \approx 20$. However, much lower transmission is obtained for s-polarised light. These results support the fact that SPP excitation occurs only for p-polarized light and thus the TP-SPP coupling process is physically driven by the SPP excitation rules. Surprisingly, a certain transmission enhancement ($\gamma \approx 4$) is obtained for s polarised light at resonance. This effect is due to the reduction in the effective thickness of the gold layer as a result of introducing the grating.

To demonstrate this design, we fabricated structures consisting of nine DBR pairs of $\lambda/4n$ thickness Si_3N_4/SiO_2 of central wavelength $\Lambda = 660$ nm and a 120 nm thick Au film thermally evaporated over the top layer of the DBR. The DBR was grown using plasma-enhanced chemical vapor deposition on a glass substrate, and a 120 nm thick Au film was thermally evaporated on the top layer of the DBR. Reflectance measurements through the glass and DBR show a strong dip at $\lambda \approx 710$ nm (see Fig. 3(a)). Finally, several gratings of depth 30 nm were fabricated on the top surface of the metal layer using focused ion beam (FIB) etching,[28] with periods (Λ) between 500 and 700 nm and $f = 0.5$. For this study, we focus on three different periods $\Lambda_1 = 500$, $\Lambda_2 = 600$, and $\Lambda_3 = 650$ nm. Figure 1(b) shows a scanning electron micrograph image of one of the fabricated gratings with $\Lambda = 600$ nm. These parameters match those used for the theoretical study, shown earlier in this paper, and allow direct comparison between Fig. 2 and the experimental data discussed below. The samples were characterized on a custom-built Fourier image spectroscopy setup (FIS).[29] The setup consists of a white light transmission microscope with two high numerical aperture (NA = 0.75) objective lenses as condenser and collection, respectively. A 4f configuration is used to image the back focal plane of the collection objective onto a CCD where images of the far field scattering pattern of the sample may be recorded. By raster scanning this image with a fibre-coupled spectrometer it is possible to obtain a quantitative measurement of the angular reflectance/transmittance in a specular configuration.[30] Figure 1(a) shows a schematic of the illumination/collection configuration for a particular angle θ. Raw transmission measurements of the samples were normalized by the transmission of a bare substrate (fused glass) in order to avoid spurious features in the study of the optical properties of our samples. For this experiment, we were able to resolved angular transmission patterns for $10 \times 10\ \mu$m sized gratings.

Figure 3(a) shows transmission measured for a grating of $\Lambda = 600$ nm at $\theta_{in} = 6^\circ$ for both polarizations. A maximum in transmission at $\lambda = 707$ nm is obtained, in good agreement with our calculations in Fig. 2(c). The difference in transmission between the two polarizations is also comparable to that calculated in Fig. 2(c), showing approximately four times more transmission for p-polarised light compared to s-polarised light. The slight blue shift in the experimental results arises due to the fabrication tolerance. As observed in Fig. 3, qualitative comparison with simulation (bottom) presents an outstanding agreement. Moreover, it is evident that no TP-SPP coupling occurs for s-polarization, as the transmission peak measured perfectly matches the dispersion of the TP mode in this case. However, by examining

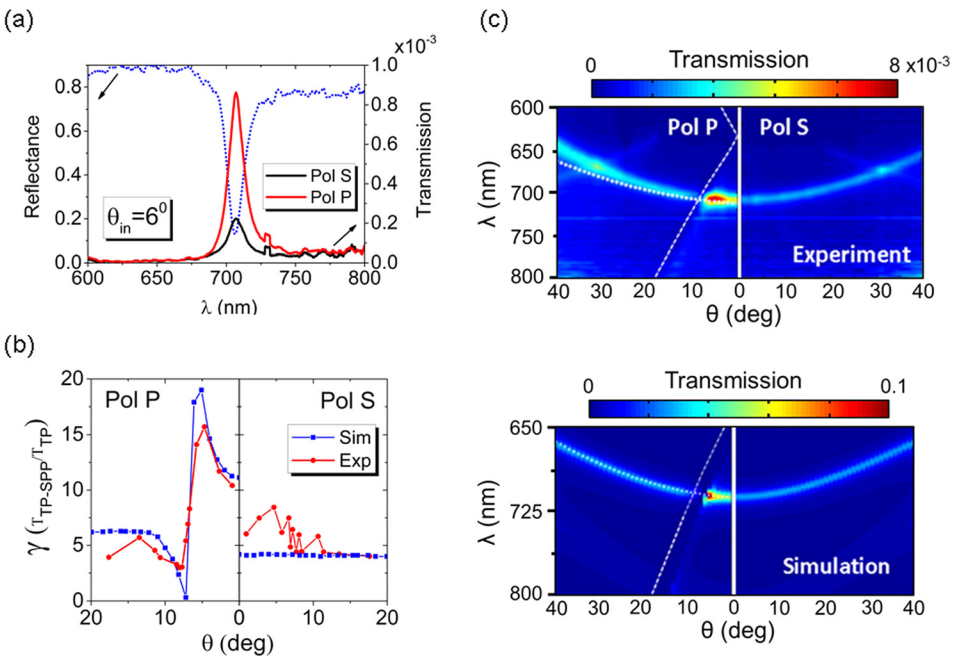

FIG. 3. (a) Normalised reflectance (blue dotted line) and transmission (solid lines) measured for the Au/DBR sample with $\Lambda = 600$ nm grating. Illumination is performed at $\theta_{in} = 6^\circ$ and for both polarizations. (b) Angle- and polarization-resolved spectral contour plots of transmission for the same sample (experiment) and parameters (simulation) than (a). White dotted (dashed) lines shows dispersion relation for TP (SPP). (c) Experiment and simulation for transmission enhancement (γ) at TP resonant wavelengths (dotted line in (b)).

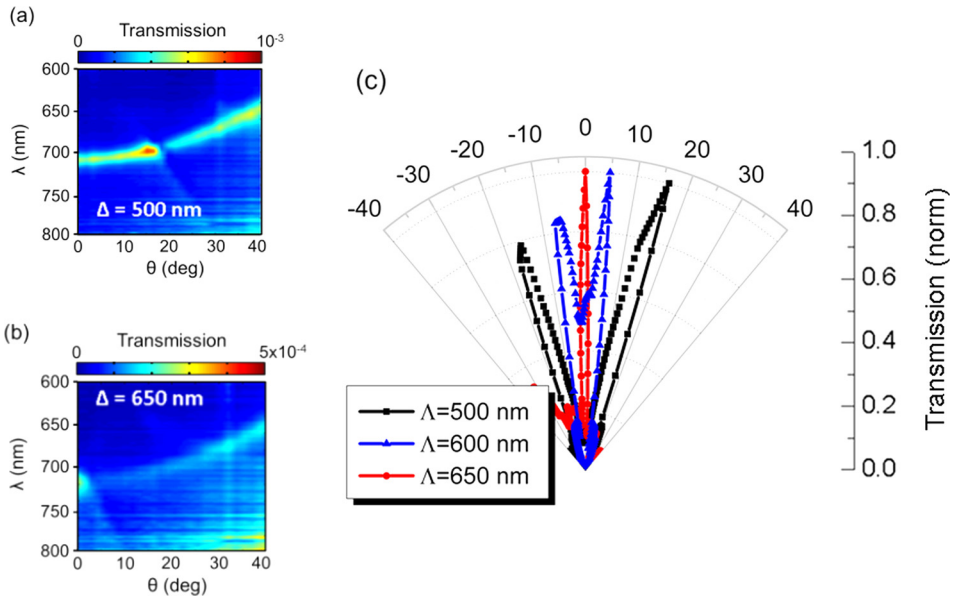

FIG. 4. (a) and (b), angle-resolved transmission for grating period $\Lambda = 500$ and 650 nm, respectively, under p-polarized illumination. (c) Polar plot for three periods $\Lambda = 500$, 600, and 650 nm at TP-TPP coupling wavelength $\lambda = 700$, 710, and 715 nm, respectively.

excitation by p-polarization, it is evident that the maximum enhancement occurs close to the angle and wavelength at which TP-SPP phase matching occurs. In order to evaluate the transmission enhancement effects, we measured a region of the sample where no grating is written. $\gamma(\omega)$ is then calculated for both polarizations as a function of the incident angle θ_{in}. Figure 3(c) shows the enhancement versus angle-of-incidence at wavelengths corresponding to the dispersion curve of the TP mode (presented by a white dotted line in Fig. 3(b)). While the simulation for s-polarization shows a constant enhancement, p polarization shows a Fano type resonance. This effect hints at the TP-SPP interaction and further decoupling to radiative modes in air.[31] In the best case ($\theta_{in} = 6°$), an enhancement of $\gamma \approx 19$ is obtained while an almost negligible transmission ($\gamma \approx 0$) occurs at $\theta_{in} = 10°$. This effect may lead to plasmon-induced total absorbance with currently increasing technological interest.[32] The measured values and trend of $\gamma(\theta_{in})$ for p-polarization presents a very good agreement with the simulated values. s-polarization does not show angular dependence for the calculated values, as expected as no SPP is excited. A slight disagreement between measurement and calculation at low angles ($\theta_{in} < 10$) is most likely related with slight misalignment of the sample relative to the incident polarization in the measurement, preventing the p-polarised enhancement from reaching the maximum predicted enhancement values. However, the outstanding agreement between measurement, calculated dispersion relations, and enhancement values as a function of angle suggest that the TP-SPP coupling process is very robust and insensitive to fabrication errors.

Although transmission enhancement is an interesting characteristic of our structure, it is evident from the previous discussion that directionality of the transmitted beam may be tuned by varying the grating period. In order to demonstrate this effect, Figs. 3(a) and 3(b) show experimental transmission contour plots for $\Lambda = 500$ and 650 nm under p-polarized illumination. Of particular interest is the period $\Lambda = 650$ nm. In that case, TP-SPP coupling takes place at almost normal incidence. This results in a normal incidence "beaming" (highly directional transmission) of the transmitted light through the sample. This phenomenon is better appreciated in Fig. 4(c), where the angle resolved transmission is polar plotted for the three different gratings ($\Lambda = 500$, 600, and 650 nm) at their particular TP-SPP coupling wavelengths ($\lambda = 700$, 710, and 715 nm, respectively). Notice that in this case transmission has been normalized by the maximum raw transmission for each period in order to make the plots comparable. As can be observed, for $\Lambda = 650$ nm, directionality of the TP-SPP coupling result in a transmitted beam with an angular tolerance of only $\Delta\theta < \pm 2°$. This effect would be technologically interesting in applications such as flat lens integrated emitting devices such as semiconductor lasers. Generally speaking, an in-depth optimization of the period for a particular application could require the choice of first- or even higher-order gratings. In that case, mode coupled theory could be the appropriate tool to obtain the best design parameters.

In conclusion, we have demonstrated that coupling between a Tamm plasmon and a surface plasmon polariton is possible for illumination from outside the system by using simple patterning on the metal layer, in contrast with complex and time-consuming fabrication techniques. We have also demonstrated that TP-SPP mode excitation can lead to enhancements in transmission of more than 16 times when compared with TP flat metal structures, no doubt of fundamental interest for applications such as single photon emission[9] or lasing[33] where TPs have already shown outstanding possibilities. Finally, tailoring of the angular pattern and polarization of the transmitted beam was shown to be possible by simply tuning the grating period. The simplicity of the device and its outstanding optical performance may be of high utility for applications, such as plasmonic-based sensors or integrated emission devices, where the presence of a metallic layer as a contact could be turned into an advantage using TP-SPP coupling.

The authors are grateful for financial support from the EPSRC Grant EP/G004366/1 and the ERC Grant No. 247462 (QUOWSS). The authors also acknowledge financial support of the Project "SPANGL4Q" of the Future and

Emerging Technologies (FET) programme within the Seventh Framework Programme for Research of the European Commission, under FET-Open Grant No. FP7-284743.

[1]I. Tamm, Z. Phys. **76**, 849 (1932).
[2]F. Ramos-Mendieta and P. Halevi, Opt. Commun. **129**, 1 (1996).
[3]A. V. Kavokin, I. A. Shelykh, and G. Malpuech, Phys. Rev. B **72**, 233102 (2005).
[4]M. Kaliteevski, I. Iorsh, S. Brand, R. A. Abram, J. M. Chamberlain, A. V. Kavokin, and I. A. Shelykh, Phys. Rev. B **76**, 165415 (2007).
[5]M. E. Sasin, R. P. Seisyan, M. A. Kaliteevski, S. Brand, R. A. Abram, J. M. Chamberlain, I. V. Iorsh, I. A. Shelykh, A. Y. Egorov, A. P. Vasil'ev, V. S. Mikhrin, and A. V. Kavokin, Superlattices Microstruct. **47**, 44 (2010).
[6]I. V. Treshin, V. V. Klimov, P. N. Melentiev, and V. I. Balykin, Phys. Rev. A **88**, 023832 (2013).
[7]W. L. Zhang and S. F. Yu, Opt. Commun. **283**, 2622 (2010).
[8]C. Symonds, A. Lemaître, P. Senellart, M. H. Jomaa, S. A. Guebrou, E. Homeyer, G. Brucoli, and J. Bellessa, Appl. Phys. Lett. **100**, 121122 (2012).
[9]O. Gazzano, S. M. de Vasconcellos, K. Gauthron, C. Symonds, P. Voisin, J. Bellessa, A. Lemaitre, and P. Senellart, Appl. Phys. Lett. **100**, 232111 (2012).
[10]R. Bruckner, M. Sudzius, S. I. Hintschich, H. Frob, V. G. Lyssenko, M. A. Kaliteevski, I. Iorsh, R. A. Abram, A. V. Kavokin, and K. Leo, Appl. Phys. Lett. **100**, 62101 (2012).
[11]W. L. Barnes, A. Dereux, and T. W. Ebbesen, Nature **424**, 824 (2003).
[12]B. I. Afinogenov, V. O. Bessonov, A. A. Nikulin, and A. A. Fedyanin, Appl. Phys. Lett. **103**, 061112 (2013).
[13]Y. Gong, X. Liu, K. Li, J. Huang, J. J. Martinez, D. Rees-Whippey, S. Carver, L. Wang, W. Zhang, T. Duan, and N. Copner, Phys. Rev. B **87**, 205121 (2013).
[14]H. Liu, X. Sun, F. Yao, Y. Pei, H. Yuan, and H. Zhao, Plasmonics **7**, 749 (2012).
[15]M. Kaliteevski, S. Brand, R. A. Abram, I. Iorsh, A. V. Kavokin, and I. A. Shelykh, Appl. Phys. Lett. **95**, 251108 (2009).
[16]G. C. Dyer, G. R. Aizin, S. J. Allen, A. D. Grine, D. Bethke, J. L. Reno, and E. A. Shaner, Nat. Photonics **7**, 925 (2013).
[17]R. Bruckner, A. A. Zakhidov, R. Scholz, M. Sudzius, S. I. Hintschich, H. Frob, V. G. Lyssenko, and K. Leo, Nat. Photonics **6**, 322 (2012).
[18]T. W. Ebbesen, H. J. Lezec, H. F. Ghaemi, T. Thio, and P. A. Wolff, Nature **391**, 667 (1998).
[19]Y. Gorodetski, N. Shitrit, I. Bretner, V. Kleiner, and E. Hasman, Nano Lett. **9**, 3016 (2009).
[20]F. J. Garcia-Vidal, L. Martin-Moreno, T. W. Ebbesen, and L. Kuipers, Rev. Mod. Phys. **82**, 729 (2010).
[21]Y. Gorodetski, A. Drezet, C. Genet, and T. W. Ebbesen, Phys. Rev. Lett. **110**, 203906 (2013).
[22]E. D. Palik, *Handbook of Optical Constants of Solids* (Elsevier, 1998).
[23]K. Crozier, V. Lousse, O. Kilic, S. Kim, S. Fan, and O. Solgaard, Phys. Rev. B **73**, 115126 (2006).
[24]J. G. Rivas, G. Vecchi, and V. Giannini, New J. Phys. **10**, 105007 (2008).
[25]Lumerical Solutions (Commercial Software), FDTD Solutions Manual Release 8.7.3. Vancouver, B.C., 2011.
[26]C.-S. Yuan, H. Tang, C. He, X.-L. Chen, X. Ni, M.-H. Lu, Y.-F. Chen, and N.-B. Ming, Physica B **406**, 1983 (2011).
[27]K. Leosson, S. Shayestehaminzadeh, T. K. Tryggvason, A. Kossoy, B. Agnarsson, F. Magnus, S. Olafsson, J. T. Gudmundsson, E. B. Magnusson, and I. A. Shelykh, Opt. Lett. **37**, 4026 (2012).
[28]Y.-L. D. Ho, R. Gibson, C. Y. Hu, M. J. Cryan, J. G. Rarity, P. J. Heard, J. A. Timpson, A. M. Fox, M. S. Skolnick, M. Hopkinson, and A. Tahraoui, J. Vac. Sci. Technol., B **25**, 1197 (2007).
[29]M. López-García, J. F. Galisteo-López, A. Blanco, J. Sánchez-Marcos, C. López, and A. García-Martín, Small **6**, 1757 (2010).
[30]J. F. Galisteo-López, M. López-García, A. Blanco, and C. López, Langmuir **28**, 9174 (2012).
[31]U. Fano, J. Opt. Soc. Am. **31**, 213 (1941).
[32]V. Yannopapas, Phys. Rev. B **73**, 113108 (2006).
[33]C. Symonds, G. Lheureux, J. P. Hugonin, J. J. Greffet, J. Laverdant, G. Brucoli, A. Lemaitre, P. Senellart, and J. Bellessa, Nano Lett. **13**, 3179 (2013).